

Complex-Difference Constrained Reconstruction for Accelerated Phase Contrast Flow Imaging

Aiqi Sun¹, Bo Zhao², Rui Li¹, and Chun Yuan^{1,3}

¹Center for Biomedical Imaging Research, School of Medicine, Tsinghua University, Beijing, China, ²Department of Electrical and Computer Engineering, University of Illinois at Urbana-Champaign, Urbana, IL, United States, ³Department of Radiology, University of Washington, WA, United States

Target audience: Scientists interested in phase contrast flow imaging

Purpose: Phase-contrast (PC) cine MRI is a promising imaging technique for studying hemodynamics. However, its clinical utility remains limited due to long acquisition time. A number of fast imaging methods have been proposed to accelerate PC cine MRI^[1], including fast data acquisition and model-based reconstruction methods. Compressed sensing combined with parallel imaging has been applied to accelerate PC flow MRI, but a potential limitation is that it could lead to inaccurate flow measurements (e.g., underestimated peak velocity) at higher acceleration factor. In this work, we propose a new complex-difference constrained reconstruction technique for accelerated PC flow imaging. We further integrate it with ESPiRiT-based parallel imaging to achieve further acceleration.

Theory & Methods: The dynamic flow images are usually highly correlated and thus can be captured by a low-rank modeling of the Casorati matrix, i.e., $C = U_s V_t$, where $U_s \in \mathbb{C}^{N \times L}$ represents the basis for the spatial subspace of C , $V_t \in \mathbb{C}^{L \times M}$ represents the basis for the temporal subspace of C , and L is the model order^[2]. Under the assumption of low-rank property in dynamic images, we can estimate the temporal subspace V_t by singular value decomposition from acquired navigation data, and then determine U_s from undersampled imaging data. The proposed reconstruction method mainly consists of the following three steps. **1) Flow-compensated image reconstruction:** We reconstruct the flow-compensated image by jointly imposing low-rank and spatial-spectral constraints^[3] as follows:

$$\langle \hat{U}_s^1, \hat{U}_s^2 \rangle = \arg \min_{U_s^1, U_s^2 \in \mathbb{C}^{N \times L}} \sum_{i=1}^{N_c} \left\| d_i - \Omega \left[F_s \sum_{j=1}^2 S_i^j (U_s^j V_t) \right] \right\|_2^2 + \lambda \sum_{j=1}^2 \left\| \text{vec}(U_s^j V_t) \right\|_1$$

Where d_i denotes the undersampled k-space data, Ω denotes the sampling operator, F_s denotes the spatial Fourier transform matrix, $S_i^j (j=1,2)$ denotes two sensitivity maps for the ESPiRiT method^[4], and λ is the regularization parameter. Then the flow-compensated image can be reconstructed based on the two sets of maps S_i^j , two spatial subspaces U_s^j and temporal subspace V_t . **2) Complex-difference images reconstruction:** Considering the spatial basis associated with the complex difference between flow-compensated image and flow-encoded images is approximately sparse, the following formulation is proposed:

$$\langle \hat{U}_{\Delta s}^1, \hat{U}_{\Delta s}^2 \rangle = \arg \min_{U_{\Delta s}^1, U_{\Delta s}^2 \in \mathbb{C}^{N \times L}} \sum_{i=1}^{N_c} \left\| \Delta d_i - \Omega \left[F_s \sum_{j=1}^2 S_i^j (U_{\Delta s}^j V_{\Delta t}) \right] \right\|_2^2 + \lambda \sum_{j=1}^2 \left\| \text{vec}(U_{\Delta s}^j V_{\Delta t}) \right\|_{TV}$$

where Δd_i denotes the k-space data difference between flow-compensated image and flow-encoded images, $V_{\Delta t}$ is calculated from the navigator data of Δd_i . **3) Reconstruction of phase difference:** We calculate the phase differences at three encoding directions by $\angle(\hat{U}_s V_t + \hat{U}_{\Delta s} V_{\Delta t}) - \angle \hat{U}_s V_t$. Fig. 1 includes a diagram that illustrates the overall reconstruction process of proposed method.

Method: To evaluate the performance of the proposed method, we collected fully-sampled data of thoracic aorta from three healthy volunteers with no symptoms of cardiovascular disease and informed written consent obtained. All scans were performed on 3.0T whole body scanner (Achieva, Philips Medical System, Best, The Netherlands) with a 32-channel cardiovascular coil. The imaging parameters were: FOV = 176×260mm² (FH/AP); slice thickness = 5mm; spatial resolution = 2.6×2.6mm²(FH/AP); flip angle = 5°; TR/TE=6.2/2.2ms; temporal resolution = 30ms; number of flow encoding directions = 3; VENC (FH/AP/RL) = 150 cm/s; cardiac synchronization: ECG-trigger. The proposed method was compared with k-t SPARSE under different reduction factors with fully-sampled central k-space data and sparsely-sampled outer k-space, and then compared based on error maps, flow profiles along time frames and root-mean-square-error (RMSE) calculations for reconstructed velocity vectors.

Results: In Fig. 2, systolic velocity maps for three directions (AP/FH/RL) reconstructed from k-t SPARSE and the proposed method under three different net acceleration factors R=4,6,8 and the reference flow-encoded images are presented. The proposed method yields higher accuracy level than k-t SPARSE. The reconstructed flow profiles along the FH-direction in the ascending aorta are shown in Fig. 3, which further illustrates improved performance of the proposed method. In contrast k-t SPARSE results in underestimation of peak velocity at R = 8.0. Fig. 4 shows that the RMSE of the reconstructed velocity vectors from the proposed method are constantly lower than k-t SPARSE algorithm.

Discussion and Conclusions: In this work, we proposed a complex-difference constrained reconstruction method to accelerate PC cine MRI. The experimental results demonstrate that the proposed method yields more accurate velocity maps than the state-of-the-art compressive sensing technique.

References: [1] Daniel Kim *et al.* MRM, 67:1054-1064, 2012; [2] Z.-P. Liang, IEEE-ISBI, 988-991, 2007; [3] B. Zhao *et al.* IEEE-TMI, 31:1809-1820, 2012; [4] Martin Uecker *et al.* MRM, 71:990-1001, 2014.

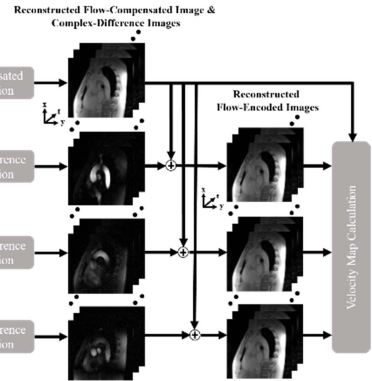


Fig. 1 The reconstruction diagram.

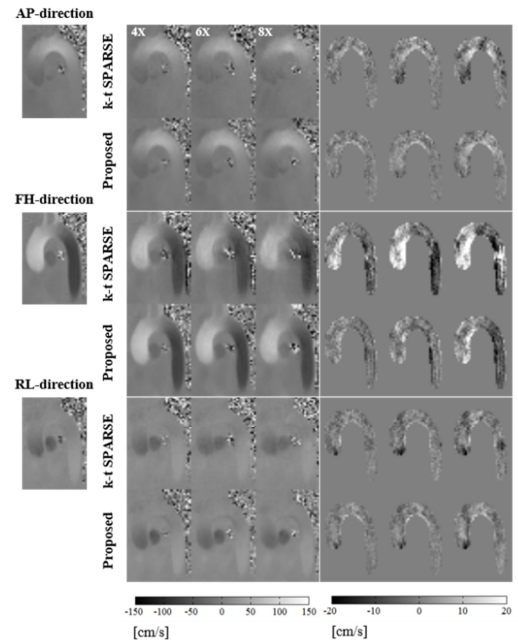


Fig. 2 Reconstructed systolic velocity maps at three directions and corresponding masked error maps for aorta region.

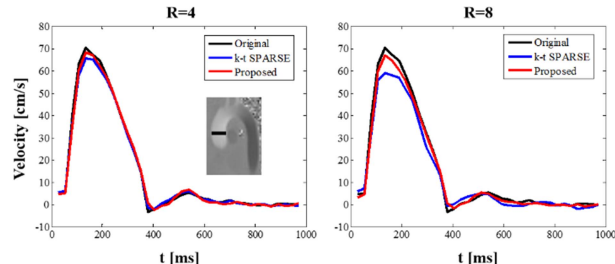


Fig. 3 Reconstructed flow profiles for a region-of-interest in ascending aorta.

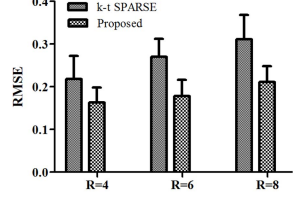


Fig. 4 The RMSE for reconstructed velocity vectors.